JACS
JOURNAL OF THE AMERICAN CHEMICAL SOCIETY

Subscriber access provided by ISTANBUL TEKNIK UNIV

Article

Synergy between Crystal Strain and Surface Energy in Morphological Evolution of Five-Fold-Twinned Silver Crystals

Weijia Zhang, Yan Liu, Ronggen Cao, Zhenhua Li, Yahong Zhang, Yi Tang, and Kangnian Fan

J. Am. Chem. Soc., **2008**, 130 (46), 15581-15588 • DOI: 10.1021/ja805606q • Publication Date (Web): 25 October 2008

Downloaded from http://pubs.acs.org on February 8, 2009

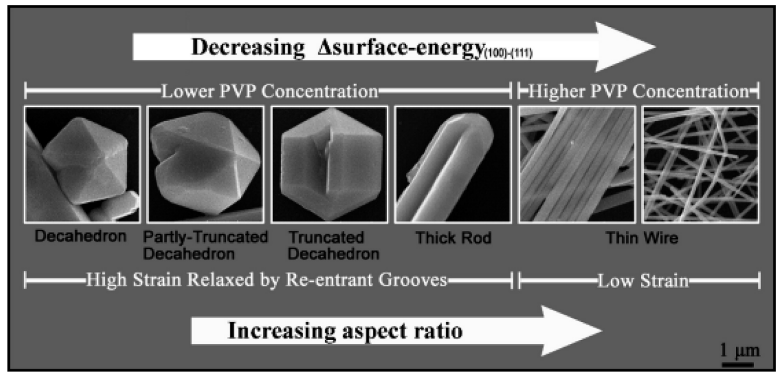

More About This Article

Additional resources and features associated with this article are available within the HTML version:

- Supporting Information
- Access to high resolution figures
- Links to articles and content related to this article
- Copyright permission to reproduce figures and/or text from this article

View the Full Text HTML

ACS Publications
High quality. High impact.

Journal of the American Chemical Society is published by the American Chemical Society. 1155 Sixteenth Street N.W., Washington, DC 20036

J|A|C|S
ARTICLES

Published on Web 10/25/2008

Synergy between Crystal Strain and Surface Energy in Morphological Evolution of Five-Fold-Twinned Silver Crystals

Weijia Zhang,[†] Yan Liu,[‡] Ronggen Cao,[§] Zhenhua Li,[‡] Yahong Zhang,[†] Yi Tang,*[,†] and Kangnian Fan[‡]

Laboratory of Advanced Materials and Center for Theoretical Chemical Physics, Department of Chemistry, Shanghai Key Laboratory of Molecular Catalysis and Innovative Materials, and Department of Materials Science, Fudan University, Shanghai 200433, People's Republic of China

Received July 18, 2008; E-mail: yitang@fudan.edu.cn

Abstract: In polyol synthesis at relatively low concentrations of polyvinylpyrrolidone (PVP, surface-capping agent), some micrometer-size Ag truncated decahedra with five-fold-twinned structure were clearly observed. This result indicates that the internal strain in the five-fold-twinned crystals is not sufficient to restrict their lateral growth. On the basis of first-principles calculation of their surface energies before and after the adsorption of surface-capping agent, it is proposed that the surface energy difference between the (100) and (111) facets ($\Delta\varphi_{(100)-(111)}$) plays an essential role in the aggressive growth of lateral (100) facets, overcoming the strain restriction. When enough PVP is adsorbed on the surfaces of Ag crystals, the $\Delta\varphi_{(100)-(111)}$ will evidently decrease, and then the strain restriction on the lateral growth becomes predominant, resulting in pentagonal anisotropic structures. Following this mechanism, diameter-tunable Ag wires have been synthesized by controlling the axial growth and the lateral growth separately at higher and lower PVP concentrations, respectively.

Introduction

Research on the formation mechanism and morphology evolution of face-centered-cubic (FCC) crystals of noble metals has become an attractive field, receiving much attention because of the unique optical, electrical, mechanical, and chemical properties of such crystals.[1,2] Following a facile scheme, polyol synthesis, which is achieved through the reduction of noble metal salts with ethylene glycol (EG) in the presence of the surface-capping agent polyvinylpyrrolidone (PVP), provides a powerful way to fabricate noble metal crystals with various morphologies.[3,4] Among the various FCC noble metal structures, pentagonal five-fold-twinned crystals have been studied for over 50 years, not only for their wide and promising applications but also due to their prominent noncrystallographic symmetry.[5] Two common morphologies of five-fold-twinned crystals have been widely studied: the regular decahedron and the pentagonal wire/rod.[1c] In the 1960s, Ino et al.[6] proposed a third morphology of truncated decahedra on the basis of free energy calculations, but the prediction applied only for small clusters and has not been observed for large colloidal crystals. Meanwhile, it was believed that five-fold-twinned crystals did not experience lateral growth of their large side faces because it was restricted by the inherent crystal strain.[7] Herein, we report experimental observation of truncated decahedral Ag particles 2−4 μm in diameter with re-entrant grooves, much larger than the predicted nanometer size of five-fold-twinned crystals. This gives reliable evidence of the existence of the truncated decahedral crystals and the relaxation of internal strain by opening some re-entrant grooves. The five-fold-twinned crystals can grow aggressively in the lateral direction; sometimes the lateral growth is unsymmetrical on the five faces, ascribed to the inhomogeneous distribution of the strain. Furthermore, in our previous work, polyol synthesis was modified to prepare Ag wires at higher synthetic concentrations,[8] and up to now, this has achieved the

[†] Laboratory of Advanced Materials.
[‡] Center for Theoretical Chemical Physics.
[§] Department of Materials Science.

(1) (a) Wang, Z. *Nanowires and Nanobelts—Materials, Properties and Devices*, 1st ed.; Tsinghua University Publishing Co.: Beijing, 2004. (b) Rao, C. N. R.; Govindaraj, A. *Nanotubes and Nanowires*; RSC on series Nanoscience; Royal Society of Chemistry: London, 2006. (c) Tao, A. R.; Habas, S.; Yang, P. *Small* **2008**, *4*, 310. (d) Xiong, Y. J.; Xia, Y. N. *Adv. Mater.* **2007**, *9*, 3385. (e) Xia, Y. N.; Yang, P. D.; Sun, Y. G.; Wu, Y. Y.; Mayers, B.; Gates, B.; Yin, Y. D.; Kim, F.; Yan, Y. Q. *Adv. Mater.* **2003**, *15*, 353. (f) Rao, C. N. R.; Vivekchand, S. R. C.; Biswasa, K.; Govindaraja, A. *Dalton Trans.* **2007**, *34*, 3728.

(2) (a) Hong, B. H.; Bae, S. C.; Lee, C. W.; Jeong, S.; Kim, K. S. *Science* **2001**, *294*, 348. (b) Wiley, B.; Sun, Y.; Xia, Y. *Acc. Chem. Res.* **2007**, *40*, 1067. (c) Wiley, B.; Sun, Y.; Mayers, B.; Xia, Y. *Chem.—Eur. J.* **2005**, *11*, 454. (d) Xiong, Y.; Xia, Y. *Adv. Mater.* **2007**, *19*, 3385. (e) Wu, B.; Heidelberg, A.; Boland, J. J.; Sader, J. E.; Sun, X. M.; Li, Y. D. *Nano Lett.* **2006**, *6*, 468.

(3) (a) Ducamp-Sanguesa, C.; Herrera-Urbina, R.; Figlarz, M. *J. Solid State Chem.* **1992**, *100*, 272. (b) Fiévet, F.; Lagier, J. P.; Figlarz, M. *MRS Bull.* **1989**, *14*, 29. (c) Fiévet, F.; Lagier, J. P.; Blin, B.; Beaudoin, B.; Figlarz, M. *Solid State Ionics* **1989**, *32/33*, 198.

(4) (a) Sun, Y.; Yin, Y.; Mayers, B. T.; Herricks, T.; Xia, Y. *Chem. Mater.* **2002**, *14*, 4736. (b) Wiley, B.; Sun, Y.; Mayers, B.; Xia, Y. *Chem. Eur. J.* **2005**, *11*, 454.

(5) (a) Hofmeister, H. *Cryst. Res. Technol.* **1998**, *33*, 3. (b) Johnson, C. L.; Snoeck, E.; Ezcurdia, M.; Rodriguez-Gonzalez, B.; Pastoriza-Santos, I.; Liz-Marzan, L. M.; Hytch, M. J. *Nat. Mater.* **2008**, *7*, 120. (c) Tao, A.; Kim, F.; Hess, C.; Goldberger, J.; He, R. R.; Sun, Y. G.; Xia, Y. N.; Yang, P. D. *Nano Lett.* **2003**, *3*, 1229. (d) Pastoriza-Santos, I.; Sanchez-Iglesias, A.; de Abajo, F. J. G.; Liz-Marzan, L. M. *Adv. Funct. Mater.* **2007**, *17*, 1443.

(6) (a) Ino, S. *J. Phys. Soc. Jpn.* **1966**, *21*, 346. (b) Ino, S.; Ogawa, S. *J. Phys. Soc. Jpn.* **1967**, *22*, 1365.

(7) Lofton, C.; Sigmund, W. *Adv. Funct. Mater.* **2005**, *15*, 1197.

 © 2008 American Chemical Society

highest output of Ag wires among various solution methods. It was also found that pentagonal five-fold-twinned Ag wires are much easier to form than those of any other noble metal. Therefore, research on the formation of five-fold-twinned Ag crystals should be valuable and representative for understanding and directing the evolution of FCC noble metal (Ag, Au, Pd, Pt, etc.) crystals with five-fold-twinned structure in wet-chemistry synthesis.

All these experimental observations are highly significant for the investigation of the shape evolution of five-fold-twinned crystals. In the polyol synthesis, the surface-capping agent PVP plays a key role, decreasing the surface energy difference of pentagonal Ag crystals for one-dimensional (1D) anisotropic growth. When the surface energy difference between the (100) and (111) facets ($\Delta\varphi_{(100)-(111)}$) is held to a sufficiently low level by passivation from PVP, the lateral growth becomes more strain-restricted and the five-fold-twinned nanocrystals evolve into thin and long Ag wires. Otherwise, the large $\Delta\varphi_{(100)-(111)}$ results in aggressive growth of lateral (100) facets with the crystal strain relaxed by re-entrant grooves, and thereby the crystals evolve into thick Ag rods or large truncated decahedral particles, or even large decahedral particles. To prove this point, we calculated the surface energies of the (100) and (111) facets of several FCC noble metals before and after adsorption of a surface-capping agent. It is suggested that the Ag crystals have the minimum difference in surface energies between the (100) and (111) facets, which can be easily reduced to a lower level by passivation from a surface-capping agent. This explains why the formation of Ag wires is more common than for other noble metals and further confirms the above-described growth mechanism. According to this mechanism, we designed a two-step feeding method for synthesizing diameter-tunable Ag wires by controlling the axial growth and lateral growth separately at different PVP concentrations. This strategy offers an effective approach for preparing FCC metallic wires with tunable diameters to meet the different requirements for crystal size for applications in conductive polymer composites, microelectronic systems, and catalysis.

Experimental Section

Chemicals and Materials. $AgNO_3$, EG, and PVP ($M_w \approx 55\,000$) were purchased from Shanghai Chemical Reagent Co. All chemicals were used as received without further purification. Stainless steel (Grad 301) grids were obtained from Baosteel Group Corp. and were cut into small pieces before use. Their composition was Si = 1.05%, Mn = 1.05%, Cr = 17.47%, Ni = 7.18%, and Fe = 73.25%, as detected by energy-dispersive X-ray spectroscopy.

Sample Synthesis. The steel-assisted polyol synthesis at the relatively higher PVP/$AgNO_3$ ratio is the same as our previous work:[8] 10 mL of $AgNO_3$ solution (0.3 M in EG), 10 mL of PVP solution (0.45 M in EG, calculated in terms of the repeating unit), and ~1 g of small stainless steel pieces were added into a 100 mL two-necked flask, and the mixture was refluxed at 120 °C for 30 min. The mixture was then heated to 140−150 °C and kept at this temperature for at least 1 h until all $AgNO_3$ was completely reduced. For the synthesis at the relatively lower PVP/$AgNO_3$ ratio, first 5 mL of $AgNO_3$ solution (0.2 M in EG), 5 mL of PVP solution (0.3 M in EG), and stainless steel pieces were added, and the mixture was refluxed at 120 °C for 30 min. After this process, the solution was still clear. Another 20 mL of $AgNO_3$ solution (0.2 M in EG) was then added, and the mixture was heated to 150−160 °C and kept at this temperature for at least 1 h until all $AgNO_3$ was completely reduced. Throughout both procedures, an air flow of ~50 sccm was constantly bubbled into the reaction mixture and vigorous stirring was maintained. After the stainless steel pieces were removed, the product was centrifuged at 12 000 rpm for 20 min to ensure complete collection of the products and then washed with ethanol to remove excess EG and PVP from the surfaces of the products. The washing and centrifugation procedure was repeated another two times. The purified products were preserved in ethanol for characterization.

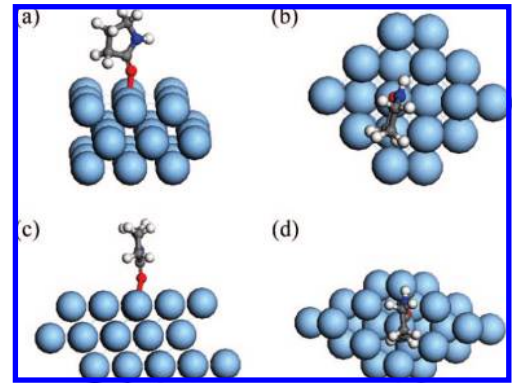

Figure 1. (a) Side view and (b) top view of a unit cell of the Ag(100) surface covered by an α-pyrrolidone molecule. (c) Side view and (d) top view of a unit cell of the Ag(111) surface covered by an α-pyrrolidone molecule. White, H; red, O; blue, N; gray, C.

The synthesis of thick Ag wires by a two-step feeding method involves the following steps. Step I: 5 mL of $AgNO_3$ solution (0.3 M in EG) and 5 mL of PVP solution (0.45 M in EG) were added into the flask. The next part was the same as the above-described steel-assisted polyol synthesis at the relatively higher PVP/$AgNO_3$ ratio until Ag wires were synthesized. The mixture was then used directly in the following process, with the as-synthesized thin Ag nanowires employed as "seeds". Step II: 10 mL of $AgNO_3$ solution (0.3 M in EG) was added into the mixture prepared in step I. The solution was heated to 150−160 °C for another 1 h. The Ag products settled after several hours; they were then washed with ethanol and redeposited (or centrifuged) several times.

Computation Details and Model. The first-principles calculations were performed within the framework of density functional theory (DFT) using the *ab initio* total energy and molecular dynamics program VASP with plane wave basis sets.[9] The exchange-correlation functional utilized is the local density approximation with generalized gradient correction, known as GGA-PW91.[10] The kinetic cutoff energy used is 300 eV. The electron-ion interaction is represented by optimized Vanderbilt ultrasoft pseudopotentials,[11] which were supplied by Kresse and Hafner.[12] The *k*-points sampling was generated following the Monkhorst−Pack procedure with a 3 × 3 × 1 mesh.

In the case of Ag, the Ag(100) and Ag(111) surfaces are modeled by a 3 × 3 supercell with a three-layer slab and a vacuum region of more than 25 Å thickness. An α-pyrrolidone is placed on the surface with a C═O end-on adsorption to give a simplified model of the PVP adsorbed on the surface. The N atoms in α-pyrrolidone/PVP have no interaction with Ag atoms on the surface because of electrostatic repulsion and spatial hindrance; for more information about the model simplification and interaction between Ag and α-pyrrolidone/PVP, see the Supporting Information. Figure 1 illustrates the 3 × 3 three-layer slab covered by an α-pyrrolidone.

(8) Zhang, W. J.; Chep, P.; Gao, Q. S.; Zhang, Y. H.; Tang, Y. *Chem. Mater.* **2008**, *20*, 1699.

(9) (a) Kresse, G.; Hafner, J. *Phys. Rev. B* **1993**, *47*, 558. (b) Kresse, G.; Hafner, J. *Phys. Rev. B* **1994**, *49*, 14251.

(10) (a) Perdew, J. P.; Chevary, J. A.; Vosko, S. H.; Jackson, K. A.; Pederson, M. R.; Singh, D. J.; Fiolhais, C. *Phys. Rev. B* **1992**, *46*, 6671. (b) Perdew, J. P.; Wang, Y. *Phys. Rev. B* **1992**, *45*, 13244.

(11) Vanderbilt, D. *Phys. Rev. B* **1990**, *41*, 7892.

(12) Kresse, G.; Hafner, J. *J. Phys.-Condes. Matter* **1994**, *6*, 8245.

Both the adsorbed molecule and the upper two silver layers are allowed to relax with the bottom-layer silver atoms fixed at their bulk positions and an optimized lattice constant of 4.18 Å.[13]

The surface energy (φ) of a pure surface is calculated according to the following expression:

$$\phi = [(E_{\text{supercell}} - nE_{\text{bulk}}) - (E_{\text{slab}} - nE_{\text{bulk}})/2]/N_{\text{surf}}$$

In this equation, $E_{\text{supercell}}$ is the energy of the pure surface; E_{slab} is the energy of the pure surface calculated by the supercell model as indicated above but with all atoms fixed at their bulk positions, E_{bulk} is the energy of a bulk unit cell, N_{surf} is the number of the surface Ag atoms in the supercell, and n (= 27/4 in the current study) is the number of repeating bulk silver unit cells in the supercell to model the surface. For the surface covered by adsorbate, φ is calculated by

$$\phi = [(E_{\text{substrate}} - nE_{\text{bulk}}) - E_{\text{adsorbate}} - (E_{\text{slab}} - nE_{\text{bulk}})/2]/N_{\text{surf}}$$

where $E_{\text{substrate}}$ is the energy of the surface covered by the α-pyrrolidone molecule and $E_{\text{adsorbate}}$ is the energy of the isolated α-pyrrolidone molecule.

Characterization. Scanning electron microscopy (SEM) images were obtained on a Philips XL 30 instrument. Transmission electron microscopy (TEM) images were obtained on a JEOL JEM-2010 instrument. In preparing the samples for microscopy, the products, which did not need further purification, were well suspended in the ethanol by ultrasonic dispersion. The ethanol suspensions of the products were dropped on a glass substrate for SEM and on copper grids coated with amorphous carbon film for TEM. The powder X-ray diffraction (XRD) pattern was obtained on a Rigaku D/MAX-rB diffractometer with Cu Kα radiation at 40 kV and 60 mA. The sample was dried under at 60 °C for 24 h before characterization. A conductive device using Ag wire and two Pt pads was fabricated on a Quanta 200 3D Focused Ion Beam to measure the electrical properties of Ag wire. Its electrical resistance and allowable current/voltage were measured on the CSM/Win family of $C-V/I-V$ plotters.

Results and Discussion

Truncated Decahedron. Two kinds of five-fold-twinned metallic crystals have been studied extensively: regular decahedra of Au[14] and Pd[15] and pentagonal wires/rods of Cu,[16] Ag,[17] Au,[18] and Pd.[19] The former is represented by a pentagonal dipyramid bounded by 10 equilateral triangle (111) facets. The latter is the corresponding elongated shape bounded by five (111) top facets, five (111) bottom facets, and five (100) lateral facets,[20] whose aspect ratios varied in a broad range usually higher than several tens. In products of the polyol synthesis at the relatively lower PVP concentration described in this paper, we successfully observed the third five-fold-twinned structure of the silver truncated decahedron (Figure 2). This morphology looks just like a pentagonal dipyramid truncated in the lateral (100) directions at a distance corresponding to the Wulff construction, resulting in the exposure of five new (100) facets and the formation a pentagonal prism between two pyramids. The existence of this morphology has been predicted on the basis of the free energy calculation as Ino decahedron,[7] which is distinguished from both a regular decahedron and a pentagonal wire by the different side faces. The side (100) facets of the truncated decahedra (Ino decahedra) have aspect ratios close to 1 (i.e., more quasi-spherical), while the side (100) facets of the pentagonal wires have high aspect ratios of tens, and the regular decahedra have no (100) facet at all. The SEM images illustrate that these synthetic truncated decahedral particles usually have a size of 2−4 μm, much larger than the nanometer size predicted by thermodynamic models.[6]

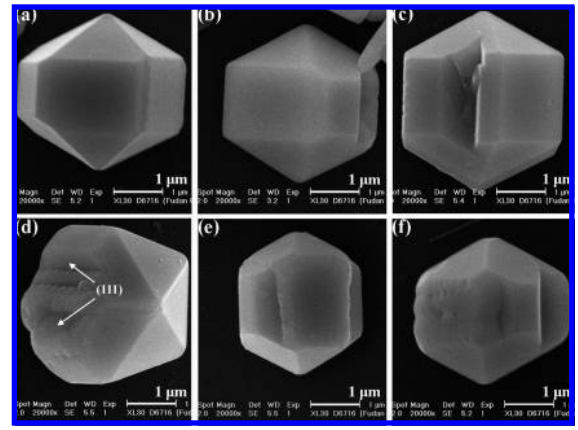

Figure 2. SEM images of Ag truncated decahedra with micrometer size, formed by the polyol synthesis. In (b)−(f), the truncated decahedra show one or several re-entrant grooves on the side faces parallel to the axial direction.

Crystal Strain and Re-entrant Groove. The experimental results give evidence for pentagonal crystals with large side faces and thick diameters, which were previously proposed to not exist. The large crystals are usually highly defective. It is well known that the regular decahedron can be considered as the junction of five tetrahedral subunits sharing one common edge along a five-fold axis (each tetrahedron is bounded by four (111) facets). Because the theoretical angle between two planes of a tetrahedron is 70.53°, five subunits cannot form a complete space-filling decahedron. The pseudo-five-fold symmetric decahedron remains unclosed by an angle of 7.35°, resulting in some form of internal strain.[21] Ascribed to the same pentagonal five-fold-twinned configurations, this strain also occurs with pentagonal wires and truncated decahedra. In principle, their lateral growth increases the strain: the greater the distance from the central axis, the higher the strain. Thus, it was proposed that five-fold-twinned crystals preferentially grow in the axial direction, which does not increase the strain.[8,22] However, the internal crystal strain may also be effectively relaxed through splitting re-entrant grooves on side faces,[23] which has been observed on a nanosized Si decahedron.[24] Herein, the wedge-shape re-entrant grooves (gaps) are very common on the micrometric truncated decahedral Ag crystals, and more details can be clearly observed, such as the locations, the angles, the depths, the number, and the plane orientation.

(13) Jia, L. L.; Wang, Fan, K. N. *J. Phys. Chem. B* **2003**, *107*, 3813.
(14) Sanchez-Iglesias, A.; Pastoriza-Santos, I.; Perez-Juste, J.; Rodriguez-Gonzalez, B.; de Abajo, F. J. G.; Liz-Marzan, L. M. *Adv. Mater.* **2006**, *18*, 2529.
(15) Lim, B.; Xiong, Y.; Xia, Y. *Angew. Chem.* **2007**, *46*, 9279.
(16) Lisiecki, I.; Filankembo, A.; Sack-Kongehl, H.; Weiss, K.; Pileni, M. P.; Urban, J. *Phys. Rev. B* **2000**, *61*, 4968.
(17) Graff, A.; Wagner, D.; Ditlbacher, H.; Kreibig, U. *Eur. Phys. J. D* **2005**, *34*, 263.
(18) (a) Johnson, C.; Dujardin, E.; Davis, S.; Murphy, C. *J. Mater. Chem.* **2002**, *12*, 1765. (b) Liu, X. G.; Wu, N. Q.; Wunsch, B. H.; Barsotti, R. J.; Stellacci, F. *Small* **2006**, *2*, 1046.
(19) Xiong, Y.; Cai, H.; Yin, Y.; Xia, Y. *Chem. Phys. Lett.* **2007**, *440*, 273.
(20) Reyes-Gasga, J.; Elechiguerra, J. L.; Liu, C.; Camacho-Bragado, A.; Montejano-Carrizales, J. M.; Yacaman, M. J. *J. Cryst. Growth* **2006**, *286*, 162.
(21) (a) Martin, T. P. *Phys. Rep.* **1996**, *273*, 199. (b) Mark, L. D. *Rep. Prog. Phys.* **1994**, *57*, 603.
(22) Melmed, A. J.; Hayward, D. O. *J. Chem. Phys.* **1959**, *31*, 545.
(23) Gryaznov, V. G.; Heydenreich, J.; Kaprelov, A. M.; Nepijko, S. A.; Romanov, A. E.; Urban, J. *Cryst. Res. Technol.* **1999**, *34*, 3.
(24) (a) Iijima, S. *Jpn. J. Appl. Phys.* **1987**, *26*, 357. (b) Iijima, S. *Jpn. J. Appl. Phys.* **1987**, *26*, 365.

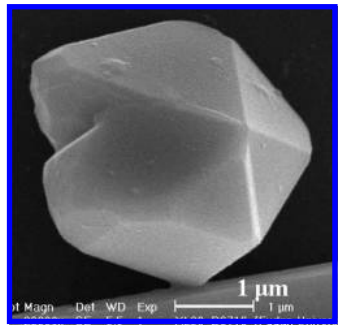

Figure 3. SEM image of a partly truncated decahedral Ag particle showing a re-entrant groove on the side.

Previously, the re-entrant grooves were supposed to be most likely localized in the twin boundaries, which are the coplane of two tetrahedral or truncated tetrahedral subunits.[21,25] However, the experimental result indicates that the most probable location is the region between two adjacent boundaries (i.e., on a single subunit) while the boundaries are kept spatially coherent, as shown in Figure 2b−f. After comparing a number of micrometric truncated decahedral particles, we found that the locations and the number of all re-entrant grooves varied from one to another, even on similarly sized particles. This suggests that the strain and the dislocation are distributed on the whole outer edges of pentagonal crystals, rather than localized at the twin boundaries or maximal at the boundaries. It is also noted that the planes of re-entrant grooves are parallel to the twin boundaries, indicating that they belong to the same facet as the boundaries, i.e., the (111) facet (indicated by white arrows in Figure 2d).

It is usually believed that the regular decahedron seeds could be "elongated" to pentagonal wires/rods if the strain restricted the lateral growth.[2d,7] However, this does not seem to be the case for truncated decahedral particles with re-entrant grooves. Probably, they are equiaxial crystals developed from the truncated decahedral nanocrystals/clusters (seeds). The first proof for this suggestion is the highly unsymmetrical morphology of a partly truncated decahedron (Figure 3), which is not explained by the process of elongation of a decahedron. This particle has some of five side edges truncated while the others are kept from being fully truncated. Second, if they were "elongated" particles resulting from internal strain, they should grow much longer. But on the contrary, they are arrested at an aspect ratio not much more or less than 1 (about 0.8−1.2), very close to a spherical shape and more in accord with the Wulff construction. Third, there is no valid effect to lead the elongation in this case. The internal strain has been effectively released by re-entrant grooves, causing the free lateral growth and the formation of quasi-spherical particles of micrometer sizes. This indicates that strain-restriction is not sufficient to induce 1D anisotropic growth. Finally, and most importantly, the stability of truncated decahedral nanocrystals is supported by the thermodynamic model.[26] The truncated decahedral configuration has a lower total surface energy than the regular decahedron.[6] Though higher energy (100) facets are exposed, the low surface/volume ratio will reduce the total surface energy. Therefore, the truncated decahedron with an approximate spherical shape is more energetically favorable than the regular decahedron. For the

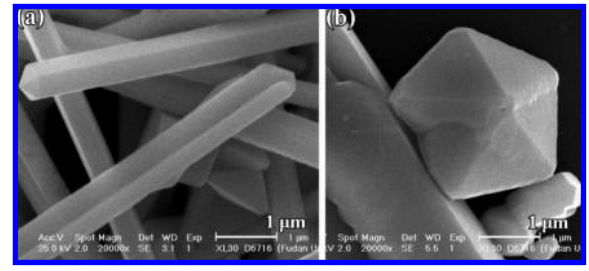

Figure 4. SEM images of a thick Ag rod (a) and a large Ag decahedron (b) with wedge-shaped re-entrant grooves.

crystals, the truncation of the sharp corners/edges is an effective approach to lower the energy. Tetrahedral, cubic, and octahedral metallic crystals also have their corner-truncated counterparts (truncated tetrahedron, cube, and octahedron) for lowering surface energies.[27]

On the other two five-fold-twinned structures of Ag wires/rods and decahedra with large size, the strain is also relaxed by opening re-entrant grooves (Figure 4). As demonstrated in Figure 4a, some Ag rods have the re-entrant grooves on their side faces along the whole wire. But the empirical results show that they seldom appear on relatively thinner wires (such as <100 nm). Re-entrant grooves are also sometimes found on the long wires, which are not as thick as particles. This may be related to the higher overall strain of wires than that of particles. Similar to the case of truncated decahedral particles, the re-entrant grooves can well accommodate the crystal strain when decahedra and wires/rods are growing larger and thicker. Thus, these pentagonal crystals with thick diameters usually show visible defects. In contrast, owing to the low strain in nanosized pentagonal crystals, the Ag nanowires seldom open re-entrant grooves on their side faces.

Lateral Growth Behavior. The thick pentagonal crystals with re-entrant grooves indicate that internal strain alone is not enough to restrict lateral growth, since the strain is relaxed by splitting re-entrant grooves. The lateral growth behavior of five-fold-twinned crystals is an interesting phenomenon which has seldom been studied before. On the basis of our experimental observations, this phenomenon is discussed below.

For the micrometric pentagonal Ag crystals, it is difficult to keep the lateral growth symmetrical, as it is in the nanometric crystals. Despite all being (100) facets, each of the five lateral facets grows unequally. Figure 5 illustrates several truncated decahedral particles that are remarkably unsymmetrical. Typically, one (or more) lateral facet of a truncated decahedron is raised in the perpendicular direction, resulting in it being farther from the central axis than the others. It looks just like a rectangular wedge section that grows out from the side (100) facet. Figure 5e,f shows front views of wedged sections. As shown in Figure 5e (white arrows), the two side faces of the wedge are extensions of the top and bottom (111) facets of the truncated decahedron, respectively. The other two faces are also (111) facets, because they are parallel to a twin boundary (a pair of parallel edges denoted by white double-lines). In another case (see Figure 5f), a side face of the overgrown wedge section is coplanar to the plane of the re-entrant groove. The unsymmetrical lateral growth, most assuredly, is highly relative to the presence of inhomogeneous strain, dislocation, and re-entrant

(25) Bogels, G.; Meekes, H.; Bennema, P.; Bollen, D. *J. Phys. Chem. B* **1999**, *103*, 7577.
(26) Barnard, A. S. *J. Phys. Chem. B* **2006**, *110*, 24498.
(27) (a) Baletto, F.; Ferrando, R. *Rev. Mod. Phys.* **2005**, *77*, 371. (b) Wiley, B.; Herricks, T.; Sun, Y.; Xia, Y. *Nano Lett.* **2004**, *4*, 1733. (c) Uyeda, R. *J. Cryst. Growth* **1974**, *24/25*, 69.

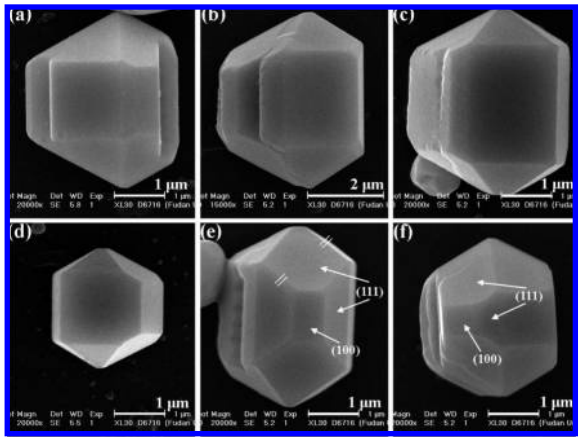

Figure 5. SEM images of Ag truncated decahedra showing unsymmetrical lateral faces. (a−d) Side views of some raised wedge sections on truncated decahedra. (e,f) Front views of another wedge sections. The white arrows indicate the (100) and (111) facets of the wedge sections. The double-lines in (e) indicate a pair of parallel edges.

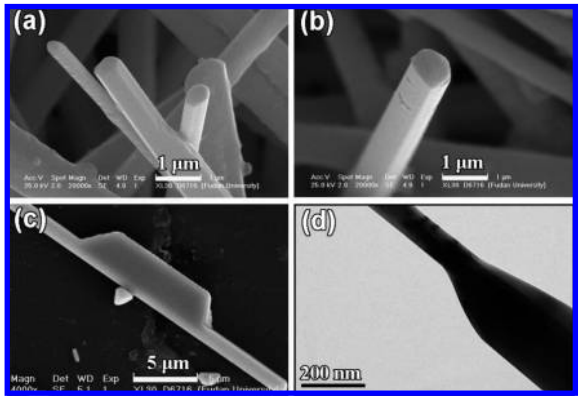

Figure 6. (a,b) SEM images of Ag wires showing the unsymmetrical cross sections. (c) SEM and (d) TEM images of Ag wires with multidiameters showing partially unsymmetrical lateral faces.

groove on or between the tetrahedral subunits. Also, it is suggested that the partly truncated decahedral particle with a re-entrant groove discussed above (Figure 3) is the result of unsymmetrical lateral growth of a truncated decahedral seed.

As expected, unsymmetrical lateral growth also occurs with the thick rods, but the details are slightly different from those for the truncated decahedra. In some cases, cross sections of rods grow into irregular shapes from the pentagon (Figure 6a,b). Another expression of unsymmetrical growth is the formation of multidiameter rods/wires (Figure 6c,d). This can be ascribed to the partial unsymmetry of a single rod/wire of which one or several segments are overgrown. The unsymmetrical cross sections are found widely in all five-fold-twinned crystals when they are growing thicker.

Evolution of Five-Fold-Twinned Ag Crystals. Compared to thick rods and large truncated decahedral particles, thin Ag wires synthesized at a relatively higher PVP concentration usually have a more symmetrical morphology. Figure 7 shows some symmetrical pentagonal wires. The umbrella-shaped tip is a pentagonal pyramid, quite similar to half of a regular decahedron, and the body is an equilateral pentagonal prism with high aspect ratio. Because of the similarity of the structure to a decahedron, pentagonal wires were previously considered to be elongated decahedra that have been lengthened parallel to their central symmetry axes. Yacaman et al.[28] proposed that their

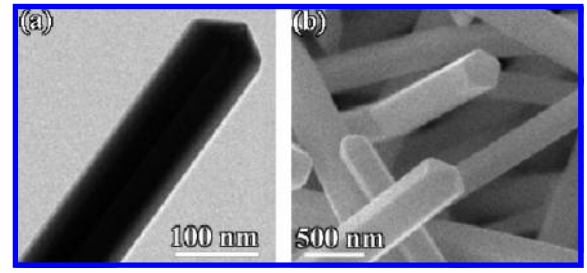

Figure 7. (a) TEM and (b) SEM images of five-fold-twinned cyclic Ag wires with regular pentagonal cross sections and umbrella-shaped tips.

diffraction pattern could be simulated as a chain of decahedra joined along the five-fold symmetry axis. Accordingly, it is generally believed that these pentagonal wires evolve from regular decahedra. However, the actual mechanism of the elongation process is still under debate. The arguments focused on two questions:

1. What causes the high-energy (100) facets to appear rather than the simple enlargement of regular decahedral seeds?

2. Under what conditions do the pentagonal crystals keep growing isotropically in all directions or anisotropically in only the axial direction?

Research on the growth of Ag wires mainly reflects two kinds of mechanisms for the elongation process. One is the soft-template mechanism, which ascribes the anisotropic growth to lateral restriction by various surface-capping agents, e.g., PVP,[29] cetyltrimethylammonium bromide (CTAB),[30] or 1,3-bis(cetyldimethylammonium)propane dibromide.[31] It is suggested that these molecules bind more strongly to (100) side facets than to (111) top facets, thus leading to the preferential deposition of atoms onto the top facets, which adsorb fewer surface-capping agents than side facets.[29,30] But this mechanism cannot answer the first question mentioned above, that is, what causes a highly symmetric decahedron (having 10 identical (111) facets with uniform surface energy) to generate five new (100) facets, instead of the equiaxial growth of 10 uniform facets. Obviously, the decahedral seeds have no (100) facets for the adsorption of surface-capping agents. Furthermore, in the case of the polyol process, it is still unclear whether PVP has a stronger affinity on a particular crystal plane.[1c,8] The soft-template mechanism tries to explain the promotion effect of organic additives on the anisotropic growth, but it does not consider the intrinsic effect of the crystal configuration. Another explanation tries to address the above two questions on the basis of the structural strain, proposing that the internal strain is largely responsible for the appearance of (100) facets and the anisotropic growth.[2d,8,21,25] In order to compensate for crystal defects, there exists some internal strain in the lattice which will be increased if atoms are located farther from the central axis. This leads to the elongation of regular decahedra in the axial direction, which does not increase the strain, while growth in the lateral direction is arrested. This strain-restriction mechanism explains the appearance of pentagonal five-fold-twinned wires independent of any particular organic additive, revealing a common cause of 1D anisotropic growth in various synthesis schemes. However, the experimental observations declared here cannot be well

(28) Elechiguerra, J. L.; Reyes-Gasga, J.; Yacaman, M. J. *J. Mater. Chem.* **2006**, *16*, 3906.
(29) Sun, Y.; Mayers, B.; Herricks, T.; Xia, Y. *Nano Lett.* **2003**, *3*, 955.
(30) Sau, T. K.; Murphy, C. J. *J. Am. Chem. Soc.* **2004**, *126*, 8648.
(31) Xu, J.; Hu, J.; Peng, C.; Liu, H.; Hu, Y. *J. Colloid Interface Sci.* **2006**, *298*, 689.

Table 1. Calculated Surface Energies of Noble Metals' (100) and (111) Facets before and after the Adsorption of α-Pyrrolidone

		φ (eV atom^{-1})		$\Delta\varphi_{(100)-(111)}$ (eV atom^{-1})		
metal	facet	clear	after adsorption of α-pyrrolidone	clear	after adsorption of α-pyrrolidone	decrease (%)
Ag	(100)	0.40724	0.39056	0.08313	0.07301	12.2
	(111)	0.32411	0.31755			
Au	(100)	0.37517	0.35724	0.11286	0.10415	7.7
	(111)	0.26231	0.25309			
Pd	(100)	0.75546	0.72117	0.25768	0.24400	5.3
	(111)	0.49778	0.47717			
Pt	(100)	0.85314	0.81504	0.35855	0.35165	1.9
	(111)	0.49459	0.46339			

explained. Some pentagonal crystals with micrometer diameters were formed at PVP concentrations lower than that used for the Ag wires synthesis. This indicates that the lateral growth cannot be effectively restricted in this condition, and the side faces still can grow extensively after the strain is relaxed. Thus, structural strain alone may be insufficient to restrict the lateral growth of pentagonal crystals. Furthermore, besides the intrinsic crystal habit, the surface-capping agents assuredly promote the formation of pentagonal wires. Particularly in the presence of PVP, the polyol synthesis of Ag wires achieves the highest yield production, but the actual effect of PVP is still to be elucidated.

The phenomena demonstrated here provide new information for the mechanism by which pentagonal crystals form and grow. Regarding question 1, it is believed that the crystals expose their (100) faces to show a truncated decahedral morphology, decreasing the total surface energy. The more spherical shape is more energetically favorable than the regular decahedron.[26] Concerning question 2—why pentagonal crystals continuously either elongate or enlarge—we suggest that it should be determined by the synergy between the crystal strain and the decrease of $\Delta\varphi_{(100)-(111)}$. Restriction due to strain in the crystals is a negative factor for the lateral growth of (100) facets, while the $\Delta\varphi_{(100)-(111)}$ is a positive factor for it. The adsorption of surface-capping agents, e.g., PVP in polyol synthesis, is a "switch" to turn down the lateral growth by suppressing the positive factor. Table 1 shows the computed surface energies of Ag crystals with and without surface-capping agents. For the convenience of calculation, the adsorption model of PVP molecules is simplified to that of α-pyrrolidone molecules. The surface energy of a clear (100) facet is 0.40724 eV atom^{-1}, higher than the 0.32411 eV atom^{-1} surface energy of a (111) facet. After adsorption of α-pyrrolidone molecules, the surface energies decrease to 0.39056 and 0.31755 eV atom^{-1}, respectively, and the difference between them decreases by 12.2%, from 0.08313 to 0.07301 eV atom^{-1}. In the case of PVP, the decreased value of $\Delta\varphi_{(100)-(111)}$ is probably higher than that of the simplified model, because the long-chain molecule will adsorb with a higher coverage on the surface of silver. This result means that, when the amount of PVP is sufficient in the synthetic system (e.g., PVP/$Ag^+ = 1.5$), it effectively passivates the crystal surfaces. The $\Delta\varphi_{(100)-(111)}$ is then dramatically reduced, and consequently the strain has the foremost influence on the crystal growth. In this situation, it is preferable to attach Ag atoms on (111) facets, which does not increase the strain. As a result, the predominant products are thin Ag wires with low strain. In the opposite situation, when the amount of PVP is insufficient, it has a smaller effect on the reduction of $\Delta\varphi_{(100)-(111)}$. As a consequence, thick or large pentagonal crystals appear in the products. For the pentagonal crystals synthesized at the relatively lower PVP concentration, the aggressive lateral growth overwhelms the strain and usually leads to re-entrant grooves for relaxing the strain. It is also prevalent for them to be unsymmetrical. However, these two particular phenomena are unwelcome for thin and small pentagonal crystals, which are not so highly strained. It is worth mentioning that PVP also acts as a protective agent, preventing aggregation, and as an assisted-reducing agent, increasing the reductive rate.[32] Thus, in polyol synthesis, the addition of PVP is quite necessary for the dispersive morphology and the reductive reaction.

In principle, it should be easy to synthesize thin pentagonal wires of other FCC noble metals through the same methods, because they have the same crystal structure. However, experiments in the literature show that they cannot be prepared with the same high output as pentagonal Ag wires, or their lengths are shorter than Ag wires. This phenomenon can be well explained by the above-described mechanism. The key to understanding this phenomenon is the different values of different noble metals' surface energies. We have also calculated the surface energies of Au, Pd, and Pt before and after adsorption of α-pyrrolidone. Their $\Delta\varphi_{(100)-(111)}$ values are much higher than that of Ag (see Table 1; for more detailed computational results, see the Supporting Information). The large differences in other noble metals cannot be decreased to a level as low as that of silver. The lowest surface energy difference explains why pentagonal wires of silver can be synthesized with the highest output and longest length among noble metals, such as Au, Pd, Pt, etc.

Generally, the $\Delta\varphi_{(100)-(111)}$ and the strain are contradictory factors affecting the attachment of atoms on lateral (100) facets. They influence the final morphology of pentagonal crystals by changing the attachment rate of atoms on lateral facets. Figure 8 shows a series of morphologies of five-fold-twinned crystals with various aspect ratios, evolving with the changing of $\Delta\varphi_{(100)-(111)}$, including a decahedron, a partly truncated decahedron, a truncated decahedron, a thick rod, and thin wires.

Secondary Lateral Growth of Ag Wires. Directed by the above-described mechanism, we planned to synthesize Ag wires having long lengths and tunable diameters by separating the 1D anisotropic growth and the lateral growth. A two-step growth strategy was designed to achieve this. In the first feeding step, $AgNO_3$ and PVP were both added into the reaction for synthesizing long wires with thin diameter and high aspect ratio. In the subsequent feeding step, only $AgNO_3$ was added again, for growth on the side faces of the wires. Figure 9a,b show thin and thick wires, respectively. The diameters of the wires increase dramatically after secondary growth. The corresponding XRD patterns reveal that the peak widths in Figure 9c are broader than those in Figure 9d, confirming the size difference.

This strategy provides an effective approach to synthesize thick FCC metallic wires with five-fold-twinned structure by using thin wires as "seeds" for the secondary growth of thick wires. Meanwhile, it further proves the above-described mechanism for the evolution of pentagonal crystals. Being competitive types of growth, the 1D anisotropic growth is required to minimize the lateral growth. Thus, it is hard to fully achieve both types of growth in one-step polyol synthesis. For example Figlarz et al., the pioneers of polyol synthesis of Ag wires, found that the high PVP/$AgNO_3$ ratio of 4 resulted in thin and long wires, while the low ratio of 1 resulted in thick and short rods.[3a] In the two-step feeding method, this conflict is addressed by

(32) Silvert, P. Y.; Tekaiaelhsissen, K. *Solid State Ion.* **1995**, *82*, 53.

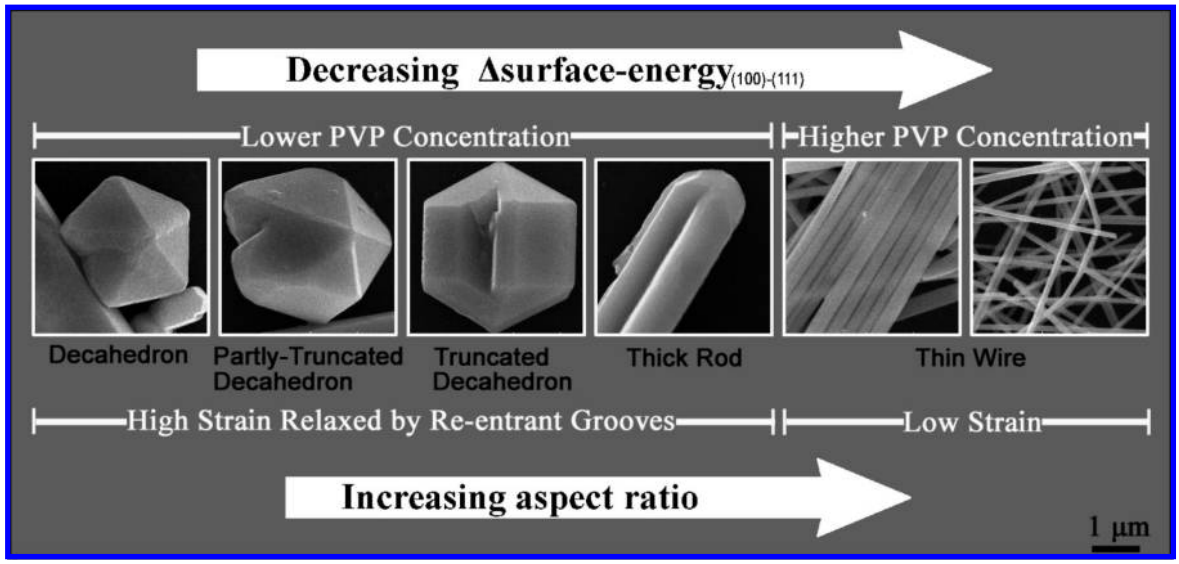

Figure 8. Scheme of the morphological diversity of five-fold-twinned silver crystals prepared by tuning synthetic condition of the polyol method.

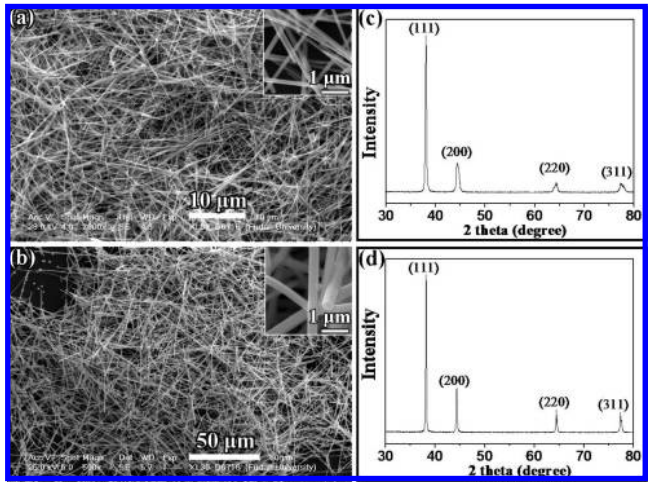

Figure 9. SEM images of Ag wires with (a) thin and (b) thick diameters and (c,d) their corresponding XRD patterns.

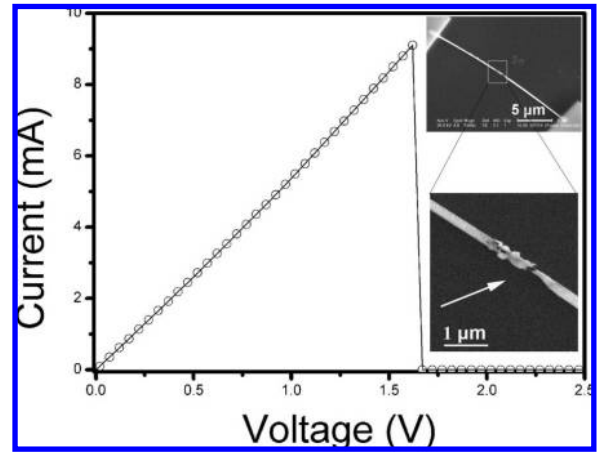

Figure 10. *I*−*V* curve of a silver wire 240 nm in diameter and 23 μm in length, prefixed with two Pt pads. Insets: SEM images of this Ag wire after fusion at relatively high current/voltage. The white arrow shows the fused gap.

separating the two types of growth. As stated above, the 1D anisotropic growth is predominant in the presence of sufficient PVP (step I), and the lateral growth is predominant at the lower PVP concentration (step II). This strategy paves the way for the syntheses of pentagonal metallic wires with tunable diameters which can be used for meeting various requirements in different practical applications.

The electrical performance of a single Ag wire has been measured by a CSM/Win family of *C*−*V*/*I*−*V* plotters. Figure 10 shows the current−voltage (*I*−*V*) curve of a single 240-nm-diameter and 23-μm-length Ag wire which is prefixed with a pair of Pt solder pads through a focused ion beam. The insets of Figure 10 display the SEM images of this Ag wire after the electrical test. A linear current−voltage curve ($I = V/178$) for this wire is obtained from Figure 10, confirming Ohm's law for the wire. It indicates that the stable ohmic resistance of this wire is about 178 Ω. The calculated conductivity is about 0.3×10^5 S/cm, which agrees with the electrical test of Ag microwires in the literature,[33] comparing to 6.2×10^5 S/cm for bulk silver materials. As shown in Figure 10, the failure of electrical conduction occurred at the maximun allowable current of 9.1 mA (current density, 2×10^7 A/cm^2) and voltage of 1.62 V. The relatively high allowable current (e.g., 9.1 mA) and voltage (e.g., 1.62 V) of the thick Ag wires make them applicable in various areas of conductive polymer composites, micro/nanodevices, and microelectronic systems.

Conclusions

Reliable evidenceis reported that the strain in five-fold-twinned crystals can be relaxed by opening some gaps on the surface. Thus, they can grow out large side faces, and sometimes the crystals are unsymmetrical on five lateral facets. When the $\Delta\varphi_{(100)-(111)}$ is decreased to a sufficiently low level by the presence of surface-capping agents, the strain restriction takes effect, leading to the 1D anisotropic growth of pentagonal crystals, and resulting in the formation of thin wires. In polyol synthesis, the adsorption of PVP on Ag crystals plays the essential role of decreasing $\Delta\varphi_{(100)-(111)}$. This study helps us understand how PVP-mediated polyol synthesis can produce pentagonal Ag wires easily and and in high yield, and it provides a typical example for the shape-controlled synthesis of metal

(33) Du, J; Han, B; Liu, Z; Liu, Y. *Cryst. Growth. Des.* **2007**, *7*, 900.

crystals. Following this formation mechanism, the preparation of long and diameter-tunable Ag wires is achieved by a secondary growth strategy, providing a general approach for the size-controlled synthesis of metallic crystals. The surface-energy-tuning strategy is expected to be useful for both single and other twinned crystals to form various shapes by controlling the growth of the crystal facets. The most important issue for this shape-controlled synthesis is to choose the right kind and amount of surface-capping agents, which have different binding abilities on crystals surfaces.

Acknowledgment. This work is supported by the NSFC (20721063, 20673026, 20673024, 20873028, and 20433020) and Major State Basic Research Development Program (2003CB615807). We thank Prof. Zhipan Liu (Fudan University) for useful discussion about the computational details and model. We are grateful to the Fudan University supercomputer center for their allocation of computer time.

Supporting Information Available: Interaction between Ag and PVP/α-pyrrolidone, model simplification, and detailed computational results. This material is available free of charge via the Internet at http://pubs.acs.org.

JA805606Q